EUROPEAN ORGANIZATION FOR NUCLEAR RESEARCH

CERN–PPE/95-154

31 October 1995

A Precise Measurement of the Tau Lepton Lifetime

DELPHI Collaboration

Abstract

The tau lepton lifetime has been measured using three different methods with the DELPHI detector. Two measurements of one-prong decays are combined, accounting for correlations, giving a result of $\tau_\tau = 291.8 \pm 3.3$ (stat.) $\pm$ 2.0(sys.) fs while the decay length distribution of three-prong decays gives the result $\tau_\tau = 286.7 \pm 4.9$ (stat.) ± 3.3 (sys.) fs. Combining the results presented here with previous DELPHI measurements, we get $\tau_\tau = 291.4 \pm 3.0$ fs and find that the ratio of the coupling constant for tau decay relative to that for muon decay is 0.990 ± 0.009, compatible with lepton universality.

(To be submitted to Physics Letters B)

P.Abreu[21], W.Adam[50], T.Adye[37], E.Agasi[31], I.Ajinenko[42], R.Aleksan[39], G.D.Alekseev[16], P.P.Allport[22], S.Almehed[24], S.J.Alvsvaag[4], U.Amaldi[9], S.Amato[47], A.Andreazza[28], M.L.Andrieux[14], P.Antilogus[9], W-D.Apel[17], Y.Arnoud[39], B.Åsman[44], J-E.Augustin[19], A.Augustinus[31], P.Baillon[9], P.Bambade[19], F.Barao[21], R.Barate[14], D.Y.Bardin[16], G.J.Barker[35], A.Baroncelli[40], O.Barring[24], J.A.Barrio[26], W.Bartl[50], M.J.Bates[37], M.Battaglia[15], M.Baubillier[23], J.Baudot[39], K-H.Becks[52], M.Begalli[6], P.Beilliere[8], Yu.Belokopytov[9,53], A.C.Benvenuti[5], M.Berggren[47], D.Bertrand[2], F.Bianchi[45], M.Bigi[45], M.S.Bilenky[16], P.Billoir[23], D.Bloch[10], M.Blume[52], S.Blyth[35], V.Bocci[38], T.Bolognese[39], M.Bonesini[28], W.Bonivento[28], P.S.L.Booth[22], G.Borisov[42], C.Bosio[40], S.Bosworth[35], O.Botner[48], B.Bouquet[19], C.Bourdarios[9], T.J.V.Bowcock[22], M.Bozzo[13], P.Branchini[40], K.D.Brand[36], T.Brenke[52], R.A.Brenner[15], C.Bricman[2], L.Brillault[23], R.C.A.Brown[9], P.Bruckman[18], J-M.Brunet[8], L.Bugge[33], T.Buran[33], T.Burgsmueller[52], P.Buschmann[52], A.Buys[9], M.Caccia[28], M.Calvi[28], A.J.Camacho Rozas[41], T.Camporesi[9], V.Canale[38], M.Canepa[13], K.Cankocak[44], F.Cao[2], F.Carena[9], P.Carrilho[47], L.Carroll[22], C.Caso[13], M.V.Castillo Gimenez[49], A.Cattai[9], F.R.Cavallo[5], L.Cerrito[38], V.Chabaud[9], Ph.Charpentier[9], L.Chaussard[25], J.Chauveau[23], P.Checchia[36], G.A.Chelkov[16], R.Chierici[45], P.Chliapnikov[42], P.Chochula[7], V.Chorowicz[9], V.Cindro[43], P.Collins[9], J.L.Contreras[19], R.Contri[13], E.Cortina[49], G.Cosme[19], F.Cossutti[46], H.B.Crawley[1], D.Crennell[37], G.Crosetti[13], J.Cuevas Maestro[34], S.Czellar[15], E.Dahl-Jensen[29], J.Dahm[52], B.Dalmagne[19], M.Dam[29], G.Damgaard[29], P.D.Dauncey[37], M.Davenport[9], W.Da Silva[23], C.Defoix[8], A.Deghorain[2], G.Della Ricca[46], P.Delpierre[27], N.Demaria[35], A.De Angelis[9], H.De Boeck[2], W.De Boer[17], S.De Brabandere[2], C.De Clercq[2], C.De La Vaissiere[23], B.De Lotto[46], A.De Min[36], L.De Paula[47], C.De Saint-Jean[39], H.Dijkstra[9], L.Di Ciaccio[38], F.Djama[10], J.Dolbeau[8], M.Donszelmann[9], K.Doroba[51], M.Dracos[10], J.Drees[52], K.-A.Drees[52], M.Dris[32], Y.Dufour[9], F.Dupont[14], D.Edsall[1], R.Ehret[17], G.Eigen[4], T.Ekelof[48], G.Ekspong[44], M.Elsing[52], J-P.Engel[10], N.Ershaidat[23], B.Erzen[43], M.Espirito Santo[21], E.Falk[24], D.Fassouliotis[32], M.Feindt[9], A.Ferrer[49], T.A.Filippas[32], A.Firestone[1], P.-A.Fischer[10], H.Foeth[9], E.Fokitis[32], F.Fontanelli[13], F.Formenti[9], B.Franek[37], P.Frenkiel[8], D.C.Fries[17], A.G.Frodesen[4], R.Fruhwirth[50], F.Fulda-Quenzer[19], J.Fuster[49], A.Galloni[22], D.Gamba[45], M.Gandelman[6], C.Garcia[49], J.Garcia[41], C.Gaspar[9], U.Gasparini[36], Ph.Gavillet[9], E.N.Gazis[32], D.Gele[10], J-P.Gerber[10], L.Gerdyukov[42], M.Gibbs[22], R.Gokieli[51], B.Golob[43], G.Gopal[37], L.Gorn[1], M.Gorski[51], Yu.Gouz[45,42], V.Gracco[13], E.Graziani[40], G.Grosdidier[19], K.Grzelak[51], S.Gumenyuk[28,53], P.Gunnarsson[44], M.Gunther[48], J.Guy[37], F.Hahn[9], S.Hahn[52], A.Hallgren[48], K.Hamacher[52], W.Hao[31], F.J.Harris[35], V.Hedberg[24], R.Henriques[21], J.J.Hernandez[49], P.Herquet[2], H.Herr[9], T.L.Hessing[9], E.Higon[49], H.J.Hilke[9], T.S.Hill[1], S-O.Holmgren[44], P.J.Holt[35], D.Holthuizen[31], S.Hoorelbeke[2], M.Houlden[22], J.Hrubec[50], K.Huet[2], K.Hultqvist[44], J.N.Jackson[22], R.Jacobsson[44], P.Jalocha[18], R.Janik[7], G.Jarlskog[24], P.Jarry[39], B.Jean-Marie[19], E.K.Johansson[44], L.Jonsson[24], P.Jonsson[24], C.Joram[9], P.Juillot[10], M.Kaiser[17], F.Kapusta[23], K.Karafasoulis[11], M.Karlsson[44], E.Karvelas[11], S.Katsanevas[3], E.C.Katsoufis[32], R.Keranen[44], Yu.Khokhlov[42], B.A.Khomenko[16], N.N.Khovanski[16], B.King[22], N.J.Kjaer[29], H.Klein[9], A.Klovning[4], P.Kluit[31], B.Koene[31], P.Kokkinias[11], M.Koratzinos[9], K.Korcyl[18], V.Kostioukhine[42], C.Kourkoumelis[3], O.Kouznetsov[13], P.-H.Kramer[52], M.Krammer[50], C.Kreuter[17], J.Krolikowski[51], I.Kronkvist[24], Z.Krumstein[16], W.Krupinski[18], P.Kubinec[7], W.Kucewicz[18], K.Kurvinen[15], C.Lacasta[49], I.Laktineh[25], S.Lamblot[23], J.W.Lamsa[1], L.Lanceri[46], D.W.Lane[1], P.Langefeld[52], I.Last[22], J-P.Laugier[39], R.Lauhakangas[15], G.Leder[50], F.Ledroit[14], V.Lefebure[2], C.K.Legan[1], R.Leitner[30], Y.Lemoigne[39], J.Lemonne[2], G.Lenzen[52], V.Lepeltier[19], T.Lesiak[36], D.Liko[50], R.Lindner[52], A.Lipniacka[36], I.Lippi[36], B.Loerstad[24], M.Lokajicek[12], J.G.Loken[35], J.M.Lopez[41], A.Lopez-Fernandez[9], M.A.Lopez Aguera[41], D.Loukas[11], P.Lutz[39], L.Lyons[35], J.MacNaughton[50], G.Maehlum[17], A.Maio[21], V.Malychev[16], F.Mandl[50], C.Maocun[2], J.Marco[41], B.Marechal[47], M.Margoni[36], J-C.Marin[9], C.Mariotti[40], A.Markou[11], T.Maron[52], C.Martinez-Rivero[41], F.Martinez-Vidal[49], S.Marti i Garcia[49], F.Matorras[41], C.Matteuzzi[28], G.Matthiae[38], M.Mazzucato[36], M.Mc Cubbin[9], R.Mc Kay[1], R.Mc Nulty[22], J.Medbo[48], C.Meroni[28], S.Meyer[17], W.T.Meyer[1], A.Miagkov[42], M.Michelotto[36], E.Migliore[45], L.Mirabito[25], W.A.Mitaroff[50], U.Mjoernmark[24], T.Moa[44], R.Moeller[29], K.Moenig[9], M.R.Monge[13], P.Morettini[13], H.Mueller[17], L.M.Mundim[6], W.J.Murray[37], B.Muryn[18], G.Myatt[35], F.Naraghi[14], F.L.Navarria[5], S.Navas[49], P.Negri[28], S.Nemecek[12], W.Neumann[52], R.Nicolaidou[3], B.S.Nielsen[29], M.Nieuwenhuizen[31], V.Nikolaenko[10], P.Niss[44], A.Nomerotski[36], A.Normand[35], W.Oberschulte-Beckmann[17], V.Obraztsov[42], A.G.Olshevski[16], A.Onofre[21], R.Orava[15], K.Osterberg[15], A.Ouraou[39], P.Paganini[19], M.Paganoni[9], P.Pages[10], H.Palka[18], Th.D.Papadopoulou[32], K.Papageorgiou[11], L.Pape[9], C.Parkes[35], F.Parodi[13], A.Passeri[40], M.Pegoraro[36], L.Peralta[21], H.Pernegger[50], M.Pernicka[50], A.Perrotta[5], C.Petridou[46], A.Petrolini[13], M.Petrovyck[28,53], H.T.Phillips[37], G.Piana[13], F.Pierre[39], M.Pimenta[21], M.Pindo[28], S.Plaszczynski[19], O.Podobrin[17], M.E.Pol[6], G.Polok[18], P.Poropat[46], V.Pozdniakov[16], M.Prest[46], P.Privitera[38], N.Pukhaeva[16], D.Radojicic[35], S.Ragazzi[28], H.Rahmani[32], J.Rames[12], P.N.Ratoff[20], A.L.Read[33], M.Reale[52], P.Rebecchi[19], N.G.Redaelli[28], M.Regler[50], D.Reid[9], P.B.Renton[35], L.K.Resvanis[3], F.Richard[19], J.Richardson[22], J.Ridky[12], G.Rinaudo[45], I.Ripp[39], A.Romero[45], I.Roncagliolo[13], P.Ronchese[36], L.Roos[14], E.I.Rosenberg[1], E.Rosso[9], P.Roudeau[19], T.Rovelli[5], W.Ruckstuhl[31], V.Ruhlmann-Kleider[39], A.Ruiz[41], H.Saarikko[15], Y.Sacquin[39], A.Sadovsky[16], G.Sajot[14], J.Salt[49], J.Sanchez[26], M.Sannino[13], M.Schimmelpfennig[17], H.Schneider[17], U.Schwickerath[17], M.A.E.Schyns[52], G.Sciolla[45], F.Scuri[46], P.Seager[20], Y.Sedykh[16], A.M.Segar[35], A.Seitz[17], R.Sekulin[37], R.C.Shellard[6], I.Siccama[31], P.Siegrist[39], S.Simonetti[39], F.Simonetto[36], A.N.Sisakian[16], B.Sitar[7], T.B.Skaali[33], G.Smadja[25], N.Smirnov[42], O.Smirnova[16], G.R.Smith[37], O.Solovianov[42], R.Sosnowski[51], D.Souza-Santos[6], E.Spiriti[40], P.Sponholz[52], S.Squarcia[13], C.Stanescu[40], S.Stapnes[33], I.Stavitski[36], F.Stichelbaut[9], A.Stocchi[19], J.Strauss[50], R.Strub[10], B.Stugu[4], M.Szczekowski[51], M.Szeptycka[51], T.Tabarelli[28],

J.P.Tavernet[23], O.Tchikilev[42], A.Tilquin[27], J.Timmermans[31], L.G.Tkatchev[16], T.Todorov[10], D.Z.Toet[31], A.Tomaradze[2], B.Tome[21], L.Tortora[40], G.Transtromer[24], D.Treille[9], W.Trischuk[9], G.Tristram[8], A.Trombini[19], C.Troncon[28], A.Tsirou[9], M-L.Turluer[39], I.A.Tyapkin[16], M.Tyndel[37], S.Tzamarias[22], B.Ueberschaer[52], O.Ullaland[9], V.Uvarov[42], G.Valenti[5], E.Vallazza[9], C.Vander Velde[2], G.W.Van Apeldoorn[31], P.Van Dam[31], W.K.Van Doninck[2], J.Van Eldik[31], N.Vassilopoulos[35], G.Vegni[28], L.Ventura[36], W.Venus[37], F.Verbeure[2], M.Verlato[36], L.S.Vertogradov[16], D.Vilanova[39], P.Vincent[25], L.Vitale[46], E.Vlasov[42], A.S.Vodopyanov[16], V.Vrba[12], H.Wahlen[52], C.Walck[44], F.Waldner[46], M.Weierstall[52], P.Weilhammer[9], C.Weiser[17], A.M.Wetherell[9], D.Wicke[52], J.H.Wickens[2], M.Wielers[17], G.R.Wilkinson[35], W.S.C.Williams[35], M.Winter[10], M.Witek[18], K.Woschnagg[48], K.Yip[35], O.Yushchenko[42], F.Zach[25], C.Zacharatou[24], A.Zalewska[18], P.Zalewski[51], D.Zavrtanik[43], E.Zevgolatakos[11], N.I.Zimin[16], M.Zito[39], D.Zontar[43], R.Zuberi[35], G.C.Zucchelli[44], G.Zumerle[36]

[1] Ames Laboratory and Department of Physics, Iowa State University, Ames IA 50011, USA
[2] Physics Department, Univ. Instelling Antwerpen, Universiteitsplein 1, B-2610 Wilrijk, Belgium
and IIHE, ULB-VUB, Pleinlaan 2, B-1050 Brussels, Belgium
and Faculté des Sciences, Univ. de l'Etat Mons, Av. Maistriau 19, B-7000 Mons, Belgium
[3] Physics Laboratory, University of Athens, Solonos Str. 104, GR-10680 Athens, Greece
[4] Department of Physics, University of Bergen, Allégaten 55, N-5007 Bergen, Norway
[5] Dipartimento di Fisica, Università di Bologna and INFN, Via Irnerio 46, I-40126 Bologna, Italy
[6] Centro Brasileiro de Pesquisas Físicas, rua Xavier Sigaud 150, RJ-22290 Rio de Janeiro, Brazil
and Depto. de Física, Pont. Univ. Católica, C.P. 38071 RJ-22453 Rio de Janeiro, Brazil
and Inst. de Física, Univ. Estadual do Rio de Janeiro, rua São Francisco Xavier 524, Rio de Janeiro, Brazil
[7] Comenius University, Faculty of Mathematics and Physics, Mlynska Dolina, SK-84215 Bratislava, Slovakia
[8] Collège de France, Lab. de Physique Corpusculaire, IN2P3-CNRS, F-75231 Paris Cedex 05, France
[9] CERN, CH-1211 Geneva 23, Switzerland
[10] Centre de Recherche Nucléaire, IN2P3 - CNRS/ULP - BP20, F-67037 Strasbourg Cedex, France
[11] Institute of Nuclear Physics, N.C.S.R. Demokritos, P.O. Box 60228, GR-15310 Athens, Greece
[12] FZU, Inst. of Physics of the C.A.S. High Energy Physics Division, Na Slovance 2, 180 40, Praha 8, Czech Republic
[13] Dipartimento di Fisica, Università di Genova and INFN, Via Dodecaneso 33, I-16146 Genova, Italy
[14] Institut des Sciences Nucléaires, IN2P3-CNRS, Université de Grenoble 1, F-38026 Grenoble Cedex, France
[15] Research Institute for High Energy Physics, SEFT, P.O. Box 9, FIN-00014 Helsinki, Finland
[16] Joint Institute for Nuclear Research, Dubna, Head Post Office, P.O. Box 79, 101 000 Moscow, Russian Federation
[17] Institut für Experimentelle Kernphysik, Universität Karlsruhe, Postfach 6980, D-76128 Karlsruhe, Germany
[18] Institute of Nuclear Physics and University of Mining and Metalurgy, Ul. Kawiory 26a, PL-30055 Krakow, Poland
[19] Université de Paris-Sud, Lab. de l'Accélérateur Linéaire, IN2P3-CNRS, Bât. 200, F-91405 Orsay Cedex, France
[20] School of Physics and Materials, University of Lancaster, Lancaster LA1 4YB, UK
[21] LIP, IST, FCUL - Av. Elias Garcia, 14-1^{o}, P-1000 Lisboa Codex, Portugal
[22] Department of Physics, University of Liverpool, P.O. Box 147, Liverpool L69 3BX, UK
[23] LPNHE, IN2P3-CNRS, Universités Paris VI et VII, Tour 33 (RdC), 4 place Jussieu, F-75252 Paris Cedex 05, France
[24] Department of Physics, University of Lund, Sölvegatan 14, S-22363 Lund, Sweden
[25] Université Claude Bernard de Lyon, IPNL, IN2P3-CNRS, F-69622 Villeurbanne Cedex, France
[26] Universidad Complutense, Avda. Complutense s/n, E-28040 Madrid, Spain
[27] Univ. d'Aix - Marseille II - CPP, IN2P3-CNRS, F-13288 Marseille Cedex 09, France
[28] Dipartimento di Fisica, Università di Milano and INFN, Via Celoria 16, I-20133 Milan, Italy
[29] Niels Bohr Institute, Blegdamsvej 17, DK-2100 Copenhagen 0, Denmark
[30] NC, Nuclear Centre of MFF, Charles University, Areal MFF, V Holesovickach 2, 180 00, Praha 8, Czech Republic
[31] NIKHEF-H, Postbus 41882, NL-1009 DB Amsterdam, The Netherlands
[32] National Technical University, Physics Department, Zografou Campus, GR-15773 Athens, Greece
[33] Physics Department, University of Oslo, Blindern, N-1000 Oslo 3, Norway
[34] Dpto. Fisica, Univ. Oviedo, C/P. Pérez Casas, S/N-33006 Oviedo, Spain
[35] Department of Physics, University of Oxford, Keble Road, Oxford OX1 3RH, UK
[36] Dipartimento di Fisica, Università di Padova and INFN, Via Marzolo 8, I-35131 Padua, Italy
[37] Rutherford Appleton Laboratory, Chilton, Didcot OX11 OQX, UK
[38] Dipartimento di Fisica, Università di Roma II and INFN, Tor Vergata, I-00173 Rome, Italy
[39] Centre d'Etudes de Saclay, DSM/DAPNIA, F-91191 Gif-sur-Yvette Cedex, France
[40] Istituto Superiore di Sanità, Ist. Naz. di Fisica Nucl. (INFN), Viale Regina Elena 299, I-00161 Rome, Italy
[41] Instituto de Fisica de Cantabria (CSIC-UC), Avda. los Castros, S/N-39006 Santander, Spain, (CICYT-AEN93-0832)
[42] Inst. for High Energy Physics, Serpukov P.O. Box 35, Protvino, (Moscow Region), Russian Federation
[43] J. Stefan Institute and Department of Physics, University of Ljubljana, Jamova 39, SI-61000 Ljubljana, Slovenia
[44] Fysikum, Stockholm University, Box 6730, S-113 85 Stockholm, Sweden
[45] Dipartimento di Fisica Sperimentale, Università di Torino and INFN, Via P. Giuria 1, I-10125 Turin, Italy
[46] Dipartimento di Fisica, Università di Trieste and INFN, Via A. Valerio 2, I-34127 Trieste, Italy
and Istituto di Fisica, Università di Udine, I-33100 Udine, Italy
[47] Univ. Federal do Rio de Janeiro, C.P. 68528 Cidade Univ., Ilha do Fundão BR-21945-970 Rio de Janeiro, Brazil
[48] Department of Radiation Sciences, University of Uppsala, P.O. Box 535, S-751 21 Uppsala, Sweden
[49] IFIC, Valencia-CSIC, and D.F.A.M.N., U. de Valencia, Avda. Dr. Moliner 50, E-46100 Burjassot (Valencia), Spain
[50] Institut für Hochenergiephysik, Österr. Akad. d. Wissensch., Nikolsdorfergasse 18, A-1050 Vienna, Austria
[51] Inst. Nuclear Studies and University of Warsaw, Ul. Hoza 69, PL-00681 Warsaw, Poland
[52] Fachbereich Physik, University of Wuppertal, Postfach 100 127, D-42097 Wuppertal 1, Germany
[53] On leave of absence from IHEP Serpukhov

1 Introduction

The tau lepton is a fundamental constituent of the Standard Model and its lifetime can be used to test the model's predictions. In particular, lepton universality can be probed using the relationships

$$\begin{aligned} \tau_\tau &= \tau_\mu \left(\frac{g_\mu}{g_\tau}\right)^2 \left(\frac{m_\mu}{m_\tau}\right)^5 \times \mathrm{BR}\left(\tau^- \to e^- \bar{\nu_e} \nu_\tau\right), \\ \tau_\tau &= \tau_\mu \left(\frac{g_e}{g_\tau}\right)^2 \left(\frac{m_\mu}{m_\tau}\right)^5 \times \mathrm{BR}\left(\tau^- \to \mu^- \bar{\nu_\mu} \nu_\tau\right) R(m_\mu/m_\tau), \end{aligned} \quad (1)$$

where $\tau_{\mu,\tau}$ and $\mathrm{m}_{\mu,\tau}$ are the lifetimes and masses of the muon and tau lepton, $\mathrm{g}_{e,\mu,\tau}$ are the coupling constants to the $W^\pm$ for the electron, muon and tau respectively and $R(m_\mu/m_\tau)$ is a phase space correction for the tau to muon branching ratio [1].

The lifetime measurements presented here were derived from the data taken by the DELPHI experiment at LEP during 1992 and 1993 at centre-of-mass energies around 91 GeV. The $\tau^+\tau^-$ data were selected in the same way as those used for the $\mathrm{Z} \to \tau^+\tau^-$ lineshape measurement [2]. As in previous measurements [3] the 3 layer single-sided silicon microvertex detector [4] and its good spatial precision are the key to making the track measurements necessary to accurately measure the short tau decay distance.

Three techniques were used to measure the lifetime. Two of them treated events where both taus decay into single charged particles, while the third one was used to study tau decays producing three charged particles. The one-prong measurements extract lifetime information from the relationship between the impact parameter and the lifetime. The third method reconstructed the decay vertex for tau leptons from the three charged particles and hence measured the flight distance from the centre of the interaction region of the LEP beams.

The Monte Carlo program KORALZ [5] was used to model tau decays in all of these analyses. This was interfaced to a detailed model of our detector response [6] to cross-check event reconstruction for biases.

The DELPHI detector is described in [7]. This analysis uses the charged particle tracking system covering the polar angle range $|\cos\theta| < 0.73$. This consists of four detectors in a 1.2 T solenoidal magnetic field:

1. the Microvertex Detector (VD) is a 3 layer single sided silicon vertex detector, consisting of 24 overlapping plaquettes per layer, which provides an $R\phi$[†] resolution of 8 μm and a two track separation of 100 μm;
2. the Inner Detector (ID) is a gas detector with a jet-chamber geometry. It produces up to 24 points per track, yielding a track element with an $R\phi$ resolution of 60 μm;
3. the Time Projection Chamber (TPC) is the main tracking detector of DELPHI, situated between radii of 30 cm and 120 cm. Up to 16 points per track produce a track element with an $R\phi$ resolution of 250 μm;
4. the Outer Detector (OD) consists of 24 modules containing 5 layers of drift tubes operating in limited streamer mode and situated at a radius of 2 m. Charged particles produce track elements with 300 μm precision in $R\phi$.

The resolution of a track extrapolation to the interaction region is dominated by the spatial resolution of the VD and its alignment precision. The relative positions of the VD

[†] R, ϕ and z define a cylindrical coordinate system, $+z$ being coincident with the electron beam and R and ϕ in the plane transverse to the beam.

modules were surveyed to an accuracy of 20 μm in three dimensions before installation in DELPHI. Movement with respect to the rest of the DELPHI detector was monitored using lasers and found to be less than 5 μm over the running period. The final alignment was carried out using tracks from Z$\rightarrow$ $\mu^+\mu^-$ decays, selected as described in [2], and tracks from Z$\rightarrow$ hadrons which cross the overlap regions of the VD modules within a single layer.

The track extrapolation resolution, $\sigma_{\rm extrap}$, can be expressed as

$$\sigma^2_{\rm extrap} \approx \sigma^2_{\rm asympt} + \left(\frac{\sigma_{\rm ms}}{p_t\sqrt{\sin\theta}}\right)^2. \qquad (2)$$

The first term is the asymptotic resolution for high momentum tracks and reflects the combination and resolution of the tracking detectors used. The second term describes the effect of multiple scattering with p_t, the transverse momentum with respect to the z axis, in GeV/c. For tracks with elements in the ID, TPC and one hit in each of the VD layers, $\sigma_{\rm asympt}$ is 23 μm and $\sigma_{\rm ms}$ is 69 μm GeV/c. A more complete discussion of the estimation of $\sigma_{\rm extrap}$ is presented in section 2.2.

The centre of the interaction region is used to estimate the tau production point. It was measured in samples of about 100 hadronic Z decays. The centre was determined in this way with a precision of 5 μm. In the $R\phi$ plane the interaction region is an ellipse with a semi-major axis of about 100 μm and a semi-minor axis of less than 10 μm.

The two one-prong measurements are described in the following section, which includes the correlations between these two measurements which use overlapping data samples. Section 3 describes the decay length analysis applied to three-prong tau decays. Finally, section 4 presents the combined result and conclusions.

2 One-Prong Lifetime Measurements

The tau sample used here was selected with the standard lineshape cuts [2], with the additional requirement that there were only two reconstructed charged tracks of opposite charge, having a transverse momentum greater than 1 GeV/c. Complementary sets of cuts were used to identify $e^+e^- \rightarrow e^+e^-, \mu^+\mu^-$ samples. These latter samples were used to measure the extrapolation resolution, monitor the track selection criteria and study the difference in tracking between electrons and muons. The data sample sizes available for each year are shown in Table 1.

Table 1: Di-lepton event samples for the 1992 and 1993 data. The tau sample only includes decays to one charged particle.

	1992	1993
$e^+e^- \rightarrow e^+e^-$	16519	17014
$e^+e^- \rightarrow \mu^+\mu^-$	16398	16179
$e^+e^- \rightarrow \tau^+\tau^-$	11542	11736

The lifetime information for one-prong tau decays is obtained by measuring the impact parameter of charged tracks, defined as the distance of closest approach of the extrapolated tracks to the production point. For tracks coming from tau decays, in case of

a perfect knowledge of the track parameters and of the production point, the impact parameter in the $R\phi$ plane is given by:

$$d = L \sin\theta_\tau \sin(\phi - \phi_\tau), \tag{3}$$

where L is the decay length, ϕ_τ the azimuthal direction of the decaying object, ϕ the track's azimuth and θ_τ the polar angle of the decaying object. The sign of the geometric impact parameter is defined as the sign of the z component of $\vec{a} \times \vec{b}$ where $\vec{a}$ is the projection on the $R\phi$ plane of the vector from the centre of the interaction region to the point, P, of closest approach and $\vec{b}$ is the track vector at P. Geometric impact parameters were used in the calculation of the resolution functions, as well as in the extraction of the tau lifetime in sections 2.1 and 2.2.

Tracks selected for these analysis, including the e^+e^- and $\mu^+\mu^-$ events used to measure the resolution functions, satisfied the following criteria:

1. at least 11 points in the TPC;
2. at least two layers with hits in the VD;
3. a χ^2 probability for the track fit in the TPC and VD greater than 0.01;
4. if the track had hits in only 2 layers of the VD, there should not be any other hit within 400 μm, in order to reduce misassociation of hits to the track.

The above selection criteria, when applied to e^+e^- and $\mu^+\mu^-$ events, showed no offset biases to the impact parameter distributions.

The background composition of the tau decay samples was determined by applying all tau selection and tracking quality cuts to simulated samples of each background class. From a sample of two million hadronic Z decays, no events were found which survived our selection. The precision tracking selection reduced the cosmic ray background to negligible levels. Other sources of background considered in the final tau sample were $e^+e^- \to e^+e^-, \mu^+\mu^-$ and two photon ($e^+e^- \to e^+e^-X$) events. The overall background levels are lower than for the normal linescan selection as our track quality cuts further reduce acollinear e^+e^- and $\mu^+\mu^-$ decays which are due to tracking defects and would otherwise end up in the tau sample. The background levels, along with the statistical uncertainties from the simulated samples used, are shown in Table 2.

Table 2: Backgrounds in the tau event samples. The uncertainties are based on the statistics of the simulated samples.

	1992	1993
$e^+e^- \to e^+e^-$	$0.22 \pm 0.06\%$	$0.28 \pm 0.06\%$
$e^+e^- \to \mu^+\mu^-$	$0.13 \pm 0.04\%$	$0.17 \pm 0.05\%$
$e^+e^- \to e^+e^-X$	$0.27 \pm 0.06\%$	$0.36 \pm 0.09\%$
Total	$0.62 \pm 0.09\%$	$0.81 \pm 0.12\%$

The tau lifetime was extracted from one-prong decays using two methods. The first method used the impact parameter difference which represents an improvement over the single hemisphere impact parameter lifetime determination (see for example [3]) by reducing the dependence of the lifetime on the unknown tau decay angle. In the impact parameter difference method the knowledge of the tau pair production point is limited by the size of the interaction region, whose dimensions are larger than the track extrapolation resolution of the detector. To overcome this, the second method used the track pair miss

distance. There the two impact parameters in a $\tau^+\tau^-$ event were summed so that the dependence on the production point inside the interaction region cancelled to first order. This second method is sensitive to the knowledge of the resolution function, which will therefore be described in detail in section 2.2. The single hemisphere impact parameter measurement, used previously, is not reported here because it is highly correlated to the above two methods and hence adds negligible precision to the lifetime measurement.

2.1 The Impact Parameter Difference Method

The impact parameter of a tau decay product is generated both by the flight distance of the decaying tau and the angle the decay track makes with the original tau direction. This can be exploited to determine the tau lifetime by correlating the impact parameters and the difference in azimuthal angles of the tau decay products.

Taking d from Eqn. 3, we can form the impact parameter difference:

$$d_+ - d_- = L_+ \sin\theta_{\tau+} \sin(\phi_+ - \phi_{\tau+}) - L_- \sin\theta_{\tau-} \sin(\phi_- - \phi_{\tau-}) \tag{4}$$

Assuming collinearity (i.e. neglecting initial and final state radiation) the taus are emitted in opposite directions giving $\phi_{\tau+} - \phi_{\tau-} = \pi$ and $\sin\theta_{\tau+} = \sin\theta_{\tau-} \equiv \sin\theta_\tau$. Averaging over decay lengths ($< L_+ > = < L_- > \equiv < L >$) and approximating $\sin(\phi_i - \phi_\tau) \approx \phi_i - \phi_\tau$, since the tau decay product follows the tau direction within a few degrees, gives

$$< d_+ - d_- > \quad = \quad < L > (\phi_+ - \phi_- + \pi) \sin\theta_\tau \quad = \quad < L > \Delta\phi \sin\theta_\tau, \tag{5}$$

where: $< L > = \beta\gamma c\tau_\tau$ is the average decay length; $\beta\gamma c = (p_\tau/m_\tau)$; c is the speed of light; p_τ is the tau momentum calculated from the beam energy taking into account radiative corrections; m_τ is the mass of the tau; and τ_τ is its lifetime. Thus the impact parameter difference, $< d_+ - d_- >$, is proportional to the projected acoplanarity ($\Delta\phi \sin\theta_\tau$ where $\Delta\phi = \phi_+ - \phi_- + \pi$) with a proportionality constant that is related to the tau lifetime.

The variables d_+, d_-, $\Delta\phi$ and θ_τ are measured on an event-by-event basis to extract the correlation, θ_τ being estimated from the direction of the thrust axis. While $\phi_\pm - \phi_{\tau_\pm}$ cannot be determined event-by-event, the decay angle difference, $\Delta\phi$, is measured with a precision of 0.5 mrad. Another advantage of this method is that backgrounds such as $\mu^+\mu^-$ or e^+e^- events tend to have small $\Delta\phi$ and hence have a reduced effect on the correlation determination. The prime drawback of this method is that $d_+ - d_-$ is doubly smeared by the lack of knowledge of the tau pair production point inside the interaction region. Moreover other backgrounds such as two photon events or radiative $\mu^+\mu^-$ and e^+e^- events have $< d_+ - d_- > \approx 0$ independent of the projected acoplanarity. This gives a bias towards smaller lifetimes.

For this analysis both tracks were required to satisfy the criteria described at the beginning of this section. Events emitting a photon due to radiative corrections to the tau production process tend to have an increased acoplanarity, biasing the measurement towards shorter lifetimes. Events with a photon of energy greater the 1 GeV having an invariant mass with the closest charged particle of more than 2 GeV/c^2 were removed, as such photons could not have originated from the tau decay. The bias due to events in which the radiated photon is softer or not detected is still not negligible and is indicated later in this section. This left 6439 events in the 1992 data sample and 6801 events in the 1993 data sample, with $|\Delta\phi \sin\theta_\tau| < 0.2$ rad, which were used for the lifetime determination.

The lifetime was extracted from an event-by-event χ^2 fit of a straight line to the variable $Y = d_+ - d_-$ as a function of $X = \frac{\beta\gamma}{(\beta\gamma)_{\rm ref}} \Delta\phi \sin\theta_\tau$. The ratio of the relativistic

factors allows the use of points taken at different beam energies by rescaling to a reference value, which was chosen to be 45.6 GeV. Each event is weighted by $1/\sigma_{\rm ipd}{}^2$, where $\sigma_{\rm ipd}$ is the quadratic sum of the extrapolation resolution $\sigma_{\rm extrap}$, the interaction region size $\sigma_{\rm ir}$, and the width of the tau decay length distribution σ_τ:

$$\sigma^2_{\rm ipd} = \sigma^2_{{\rm extrap},+} + \sigma^2_{{\rm extrap},-} + \sigma^2_{\rm ir} + \sigma^2_\tau. \tag{6}$$

The last term in this expression arises because even for perfect impact parameter resolution the impact parameter difference has a width due to the variation in decay lengths from event to event. The slope of the line was used to determine the lifetime according to Eqn. 5. The fit was iterative, removing the 0.4% of events with the greatest residuals. This procedure removed poorly reconstructed events as well as some tau decays with very long flight length. Figure 1 shows $< d_+ - d_- >$ versus X for the 1992 and 1993 data samples combined. The slopes derived from the fit were

$$L_{92} = 2.174 \pm 0.051 \text{ mm}, \tag{7}$$
$$L_{93} = 2.116 \pm 0.054 \text{ mm}, \tag{8}$$

where the uncertainties quoted are statistical only. These slopes can be converted to lifetimes using the reference value for the beam energy and the world average tau mass, 1777.1 MeV/c^2 [8], but still need to be corrected for the biases shown in Table 3.

Table 3: Summary of the systematic uncertainties and corrections in the impact parameter difference tau lifetime determination.

	1992	1993	Correlation
	fs	fs	
Simulation of Tau Production	$+5.1 \pm 0.3$	$+5.3 \pm 0.3$	1.0
0.4% Removal of Events	$+6.5 \pm 1.6$	$+8.3 \pm 1.6$	0.0
$\gamma\gamma$ Background	$+1.3 \pm 0.4$	$+1.8 \pm 0.5$	1.0
Di-leptons Background	$+0.5 \pm 0.1$	$+0.7 \pm 0.1$	0.0
Alignment	± 0.4	± 0.4	1.0
Event Selection	± 0.7	± 0.9	0.0
Tracking Resolution	± 0.5	± 0.5	1.0
Branching Ratios/Polarisation	± 0.3	± 0.3	1.0
Total	$+13.4 \pm 2.0$	$+16.1 \pm 2.0$	0.2

The violation of the collinearity assumption and the effect of radiation in the determination of the tau momentum create a bias of 5.1 ± 0.3 fs and 5.3 ± 0.3 fs in 1992 and 1993 respectively. This bias computed mainly from the simulation of tau production, including radiative effects, is common to both years' analyses. On the other hand the bias induced by removing 0.4% of the events depends on the beam spot size, which is substantially different for the two years ($+6.5 \pm 1.6$ fs and $+8.3 \pm 1.6$ fs respectively) and thus these systematic uncertainties are treated as uncorrelated from one year to the next. The systematic uncertainties include the simulation statistics and fluctuations of the lifetime determined by varying the fraction of removed event. A further small correction is due to the background contamination.

Additional systematic uncertainties arise from the vertex detector alignment (0.4 fs) corresponding to coherent changes in the radial position of the vertex detector layers of

20μm. A conservative approach is taken in assuming that these uncertainties are fully correlated from one year to the next, since possible defects in the alignment may affect the lifetime results in the same way. This procedure is adopted in all three analyses.

The effect of the event selection was computed varying the selection cuts and the r.m.s. of the fluctuation (0.7 fs for 1992 and 0.9 fs for 1993) is indicated as a systematic error. The method is also quite insensitive to the impact parameter resolution (0.5 fs), and tau branching ratios or polarisation (0.3 fs).

The slopes of Eqns. 7 and 8 correspond to tau lifetimes of:

$$\tau_{92} = 296.2 \pm 6.6 \text{ (stat.)} \pm 2.0 \text{ (sys.) fs}, \quad (9)$$

$$\tau_{93} = 291.4 \pm 7.0 \text{ (stat.)} \pm 2.0 \text{ (sys.) fs}. \quad (10)$$

These can be combined, accounting for the correlations in the systematic uncertainties shown in Table 3, to give a final result of:

$$\tau_{ipd} = 293.9 \pm 4.8 \text{ (stat.)} \pm 1.5 \text{ (sys.) fs}.$$

2.2 The Miss Distance Method

The miss distance method used both tracks in a 1-v-1 topology event, as did the impact parameter difference method. The impact parameters here were signed according to the same convention. The miss distance, d_{miss}, was given by

$$d_{miss} = d_+ + d_-, \quad (11)$$

where d_+ and d_- were defined in Eqn. 3.

Both particles in the event were required to satisfy the criteria described at the beginning of section 2. In addition we required that there be at most one other layer with an unassociated hit within 7.5° of the track in ϕ. This removed a small number of events with conversions, delta-rays and three-prong decays where the other two tracks were unassociated in the VD. This gave final sample sizes of 6506 and 6899 events for the 1992 and the 1993 data respectively.

The lifetime was estimated using an event-by-event maximum likelihood technique. The probability density function for each event was determined with an analytical convolution of a physics function and an impact parameter resolution calculated for each of the two tracks in an event. The physics function was built computing the "true" miss distance from the full Monte Carlo simulation, filtered with the same selection cuts as those used on the data sample, and parameterised with a double exponential and a Gaussian term as a function of the tau lifetime. The impact parameter resolution was parameterised as in Eqn. 2. The asymptotic term, σ_{asympt}, is proportional to the single hit precision of the VD, σ_{VD}, with the constant of proportionality determined from the radial distribution of hits associated to the track. For tracks with a single hit in each VD layer this constant is 2.8 and ranges from 1.9 to 6.6 for other hit patterns. The $\mu^+\mu^-$ and

Table 4: The effective VD hit precisions determined from di-electrons and di-muons.

σ_{VD} μm	1992	1993
electrons	8.07 ± 0.06	8.44 ± 0.07
muons	7.42 ± 0.05	8.08 ± 0.06

e^+e^- events were used to determine $\sigma_{\rm VD}$ for each year's data and the values are shown in Table 4. The multiple scattering term, $\sigma_{\rm ms}$ also depends on the radial distribution of VD hits associated with each track. With these resolutions, lifetime values of 293.8 ± 5.1 fs from the 1992 data and 282.6 ± 4.8 fs from the 1993 data were measured. The data from both years are shown in Figure 2 along with a combined fit.

In varying the event selection criteria, it was found that the lifetime changed by 1.1 fs in 1992 and 0.9 fs in 1993. To check for biases in the event selection, a sample of simulated events, with full detector effects, was selected and fitted in the same way as the data. This yielded a lifetime of 300.1 ± 1.3 fs, in good agreement with the input lifetime of 300.0 fs.

Table 5: Summary of the systematic uncertainties and corrections on the miss distance tau lifetime determination.

	1992	1993	Correlation
	fs	fs	
Event Selection	± 1.1	± 0.9	0.0
Tracking Resolution	± 2.5	± 2.7	1.0
Particle Misidentification	± 0.2	± 0.2	0.0
Background	$+1.8 \pm 0.5$	$+2.3 \pm 0.6$	1.0
Alignment	± 0.5	± 0.5	1.0
Physics Function	± 0.7	± 0.7	1.0
Branching Ratios/Polarisation	± 0.7	± 0.7	1.0
Fit Range	± 1.1	± 1.2	0.0
Total	$+1.8 \pm 3.2$	$+2.3 \pm 3.3$	0.8

An estimate of the systematic uncertainty arising from the knowledge of the resolution function was made by using e^+e^- and $\mu^+\mu^-$ events. A systematic uncertainty of 0.9 fs for the 1992 data and 0.7 fs for the 1993 data was assigned by comparing the values of $\sigma_{\rm VD}$ extracted from tracks with different VD hit patterns and by varying the multiple scattering term in Eqn. 2 by 3%, which is the uncertainty measured in the simulation and agrees with studies of the data made using the hadronic decays of the Z. A further uncertainty of 2.3 fs in 1992 and 2.6 fs in 1993 was included as a result of studying the effect of including a second Gaussian in the parameterisation of the vertex detector resolution to describe possible tails in the resolution function. These uncertainties were added in quadrature and attributed to our understanding of the resolution in Table 5. The fitting program applied the vertex detector resolution determined from muons to decay tracks identified as charged hadrons or muons while it applied the resolution determined from electrons to decay tracks identified as electrons[‡]. The residual uncertainty possible due to a misassignment of the particle type was estimated to be 0.2 fs.

The background, from $e^+e^-, \mu^+\mu^-$ and two photon events, listed in Table 2, was accounted for by adding to the physics function suitably normalised delta functions having zero miss distance. This resulted in 1.8 ± 0.5 and 2.3 ± 0.6 fs corrections to the lifetimes for each year's measurement. Residual alignment uncertainty (0.5 fs) and parameterisation of the physics function (0.7 fs) were additional contributions to the systematic uncertainty on the lifetime.

[‡]The particle identification used is similar to that described in ref. [9].

The uncertainty in the mean tau longitudinal polarisation was estimated by varying the weak mixing angle (θ_W) in KORALZ and found to contribute 0.3 fs to the overall lifetime systematic uncertainty, while correlations between the transverse spin components were estimated using KORALB [10] to give an uncertainty of less than 0.4 fs. An uncertainty of 0.5 fs was determined to come from possible variations in the tau branching ratios. Combining these three effects, a total systematic of 0.7 fs was assigned.

The range over which the fit was performed was chosen, after studying the data and fully simulated Monte Carlo events, to be ± 1.5 mm. This minimised the effects of tails arising from elastic hadronic scattering while preserving maximum sensitivity to the lifetime. This choice corresponded to a removal of 0.1% of the data, consistent with the amount expected from the hadronic interaction probability in the beampipe and VD. Varying the range by ± 0.5 mm introduced a further uncertainty of 1.1 and 1.2 fs to the lifetime measurements in 1992 and 1993 respectively.

The different systematic uncertainties (summarised in Table 5) were added together in quadrature, giving the following results for the tau lepton lifetime:

$$\tau_{92} = 295.6 \pm 5.1 \text{ (stat.)} \pm 3.2 \text{ (sys.) fs}, \quad (12)$$

$$\tau_{93} = 284.9 \pm 4.8 \text{ (stat.)} \pm 3.3 \text{ (sys.) fs}. \quad (13)$$

These two measurements were combined, accounting for the correlations in the systematic uncertainties shown in Table 5, to give the result

$$\tau_{md} = 290.1 \pm 3.5 \text{ (stat.)} \pm 3.1 \text{ (sys.) fs}.$$

2.3 Combination of One-Prong Measurements

Table 6: Summary of the lifetime uncertainties on the two one-prong measurements and their correlations.

	IPD	MD	Correlation
	fs	fs	
Lifetime value	293.9	290.1	-
Statistical Uncertainty	4.8	3.5	0.3
Event Selection	0.6	0.7	1.0
Removal of Events	1.1	-	-
Fit Range	-	0.8	-
Background	0.5	0.6	1.0
Tracking Resolution	0.5	2.6	1.0
Alignment	0.4	0.5	1.0
Branching Ratios/Polarisation	0.3	0.7	1.0
Particle Misidentification	-	0.1	-
Physics Function	-	0.7	-
Simulation of Tau Production	0.3	-	-
Total Uncertainty	5.0	4.7	0.32

In the combination of the one-prong measurements the correlation both in the statistical and systematic errors has to be taken into account.

The correlation between the statistical uncertainties was determined dividing the Monte Carlo simulation into sixty sub-samples and performing the miss distance and

impact parameter difference lifetime measurements on each sub-sample. The resulting fit values were then compared and the correlation extracted. The obtained value was 30%; varying the statistical correlation between 20% and 40% changes the overall uncertainty on the combined lifetime determination by less than 0.1 fs.

The systematic errors and their correlations are summarised in Table 6. The main differences in the size of the errors are due to the larger sensitivity of the miss distance method to the tracking resolution and to physics effects. In the miss distance analysis, the lifetime is obtained by subtracting $\sigma_{\rm extrap}$ from the width of the observed distribution; in the impact parameter difference analysis, $\sigma_{\rm extrap}$ affects only the relative weight of the events but does not influence the expectation value of the variable Y. The miss distance analysis is sensitive to the modelling of tau decays; the impact parameter difference does not need any assumption on the decay angle distribution.

The larger systematic uncertainties in the miss distance analysis are compensated by the smaller statistical uncertainty. Thus in the final result the two measurements contribute almost equally. Combining the results and allowing for the total correlation of 32% gives

$$\tau_{1prong} = 291.8 \pm 3.3 \text{ (stat.)} \pm 2.1 \text{ (sys.) fs.}$$

3 The Decay Vertex Reconstruction Method

Decays of the tau with three charged particles in the final state have been used to measure the lifetime by reconstructing the secondary vertex and calculating the distance from the production point of the tau. Only events where the opposite tau decays into a single charged particle are considered. To suppress hadronic background the three charged tracks were required to be consistent with having come from a single decay point (see below), have an invariant mass less than 2 GeV/c^2 and have a largest opening angle in the $R\phi$ plane of less than 0.2 radians. Photon conversions were suppressed by demanding the invariant mass of pairs of oppositely charged particles be greater than 50 MeV/c^2. A study of simulated data showed that a purity of $99.6 \pm 0.2\%$ was obtained.

Tracks were reconstructed using detector elements from the VD, ID and TPC. Since the extrapolation resolution close to the interaction region is dominated by the measurement uncertainty of the VD, care was taken to describe this accurately. It was found appropriate to parameterise it as a double Gaussian which was a function of the angle at which the track crosses the silicon wafer, the distance from the diode strip, and the energy deposited in the silicon. This parameterisation improves the estimate of the VD error, in particular for particles which deposit large amounts of energy through delta rays. The track fit was extended to take into account this parameterisation. Above 0.2%, where a cut is made, the probability distribution for the track fits is flat, showing that the tracking and errors are well understood. In contrast, the probability distribution for a single Gaussian parameterisation of the VD errors ceased to be flat below 5%.

Each of the three tracks was extrapolated towards the interaction region, and allowing for error propagation and residual misalignments the most likely vertex (x_0, y_0) is found, together with its statistical uncertainty, described by the function $\mathcal{P}$, which is approximately Gaussian in both dimensions. The probability that the three tracks came from a common vertex was obtained. This distribution was flat except for a peak for probabilities below 1% which corresponds to either badly reconstructed events or background processes. These events were removed. The final data samples for 1992 and 1993 consisted of 2032 and 2447 events respectively.

An estimate of the decay length in the $R\phi$ plane (l) was obtained by maximising the log likelihood function

$$\begin{aligned} \mathcal{L}(l,\delta_x,\delta_y) &= \log \mathcal{P}(x_v,y_v;x_0,y_0) - \tfrac{1}{2}(\delta_x/\sigma_x)^2 - \tfrac{1}{2}(\delta_y/\sigma_y)^2 \\ x_v &= x_b + \delta_x + l\cos\phi \\ y_v &= y_b + \delta_y + l\sin\phi \end{aligned} \tag{14}$$

where δ_x, δ_y are offsets in the tau production point from the average beam position (x_b, y_b), and are required to be consistent with the beam profile which is parameterised by Gaussian distributions in x and y of standard deviations σ_x and σ_y respectively. The tau direction is approximated by ϕ, the azimuthal direction of the three-prong system.

The flight distance was calculated from l using the polar angle, θ, of the three-prong system's momentum. This was converted to a flight time, t, in the rest frame of the tau via the relation

$$t = \frac{l}{\beta\gamma c \sin\theta} \tag{15}$$

where $\beta\gamma$ define the boost of the tau as in the impact parameter difference method above.

For each event, the probability was calculated that a flight time, t, was seen given a mean lifetime, τ, and a measurement uncertainty described by the resolution function $\mathrm{R}(\sigma_t)$. The most likely value of τ was obtained by maximising the product of these event probabilities. The functional form for $\mathrm{R}(\sigma_t)$ was obtained from the full detector simulation where it was found that the distribution of t about the true decay time was not a simple Gaussian, but was best described by a sum of two Gaussian distributions, one of standard deviation σ_t corresponding to 93 % of the events and one of $3\sigma_t$ for the remaining 7%. A typical value for σ_t was 100 fs. Comparison of the true and estimated values for τ showed the method to be unbiased to better than 2 fs.

To allow for possible deviations from the calculated uncertainty on the decay length, a scale factor (λ) was introduced which multiplies σ_t in the likelihood fit. The decay length distribution for the 1992 and 1993 data samples along with the curve representing the best fit lifetime value is shown in Figure 3. The fit to the 1992 data yielded $\tau_{92} = 282.3 \pm 7.2$ fs, $\lambda = 1.03 \pm 0.04$, while for 1993 data $\tau_{93} = 289.3 \pm 6.5$ fs, $\lambda = 1.05 \pm 0.04$. The fit was repeated without a scale factor, with a free parameter for the percentage contribution in the second Gaussian, and for a weighed average. The largest deviations from the original fit for the 1992 and 1993 data samples were 0.2 fs and 3.9 fs respectively, which were taken as systematic errors. The larger deviation seen for 1993 data may be indicative of residual alignment effects in that year.

A correction of +1.1 fs was made to account for the 0.4 ± 0.2% hadronic background present in the sample, as estimated from simulated data. The statistical uncertainty on the size of this background contributed a systematic uncertainty on the lifetime of 0.5 fs.

The contribution from the absolute alignment of the Microvertex Detector was estimated to be 1.8 fs. The uncertainty in the calibration of θ measured by the TPC produced a systematic of 0.3 fs. Uncertainties in the effect of initial and final state radiation contribute less than 0.5 fs. These systematics are summarised in Table 7.

	1992	1993	Correlation
	fs	fs	
Fit Method	2.0	2.0	1.0
Parameterisation of Fit	0.2	3.9	0.0
Hadronic Background	0.5	0.5	0.4
VD Alignment	1.8	1.8	1.0
Polar Angle	0.3	0.3	1.0
Radiation	0.4	0.3	0.0
Total	2.8	4.8	0.6

Table 7: Systematic uncertainty contributions to the three-prong lifetime determination by source in 1992 and 1993 showing the correlation between the years. Errors are combined in quadrature to calculate the total for each year.

The lifetime determinations for 1992 and 1993 data were

$$\tau_{92} = 283.4 \pm 7.2 \text{ (stat.)} \pm 2.8 \text{ (sys.) fs}, \quad (16)$$

$$\tau_{93} = 290.4 \pm 6.5 \text{ (stat.)} \pm 4.8 \text{ (sys.) fs}. \quad (17)$$

Combining these results and allowing for correlated systematics, the tau lifetime was measured to be

$$\tau_{3prong} = 286.7 \pm 4.9 \text{ (stat.)} \pm 3.3 \text{ (sys.) fs}.$$

4 Summary and Conclusions

The lifetime of the tau has been measured with three methods. The two one-prong measurements have been combined to give a single lifetime determination from one-prong decays. Only the systematic uncertainty attributed to the alignment of the vertex detector is common between the one-prong and three-prong measurements resulting in a 4% correlation between the two results. Combining the two results by weighting them with the reciprocal of the quadratic sum of the statistical and independent systematic uncertainties and retaining the common alignment systematic uncertainty unaltered, a tau lifetime of

$$\tau_\tau = 290.3 \pm 2.7 \text{ (stat.)} \pm 1.8 \text{ (sys.) fs}$$

was obtained. Combining this with our previously published tau lifetime results of 298 ± 7 fs [3] based on the 1991 data and using a 10 % correlation between the two results to account for similarities in the alignment procedure used for the VD gives 291.4 ± 3.0 fs. This result agrees with the value of 285.7 ± 4.1 fs predicted by Eqns. 1 assuming e-μ universality ($g_e = g_\mu$), using the DELPHI measurement of the average leptonic branching ratio corrected for a massless lepton, $BR(\tau \rightarrow l\bar{\nu}\nu) = 17.50 \pm 0.25\%$ [9], and $m_\tau = 1777.1 \pm 0.4$ MeV/c^2 [8]. Alternatively the measured lifetime may be used to determine the relative strength of the coupling constants (g_τ/g_l). This ratio was found to be 0.990 ± 0.009, consistent with lepton universality.

Acknowledgements

We are greatly indebted to our technical collaborators and to the funding agencies for their support in building and operating the DELPHI detector, and to the members of the CERN-SL Division for the excellent performance of the LEP collider.

References

[1] Y.S. Tsai, Phys. Rev. **D4** (1971) 2821.
H.B. Thacker and J.J. Sakurai, Phys. Lett. **B36** (1971) 103.
[2] P. Abreu *et al.* (DELPHI Collaboration), Nucl. Phys. **B418** (1994) 403;
P. Abreu *et al.* (DELPHI Collaboration), Nucl. Phys. **B417** (1994) 3.
[3] P. Abreu *et al.* (DELPHI Collaboration), Phys. Lett. **B302** (1993) 356.
[4] N. Bingefors *et al.*, Nucl. Instr. and Meth. **A328** (1993) 447.
[5] S. Jadach, B.F.L. Ward and Z. Was, Comp. Phys. Comm. **66** (1991) 276;
S. Jadach, B.F.L. Ward and Z. Was, Comp. Phys. Comm. **79** (1994) 503.
[6] "DELSIM Reference Manual", DELPHI note 89-68, Sept. 1989, (unpublished).
[7] P. Aarnio *et al.*, (DELPHI Collaboration), Nucl. Instr. and Meth. **A303** (1991) 233.
[8] Particle Data Group, Phys. Rev. **D50** (1994) 1404.
[9] P. Abreu *et al.* (DELPHI Collaboration) CERN PPE/95-114, to be published in Phys. Lett. B.
[10] S. Jadach and Z. Was, Comp. Phys. Comm. **85** (1995) 453.

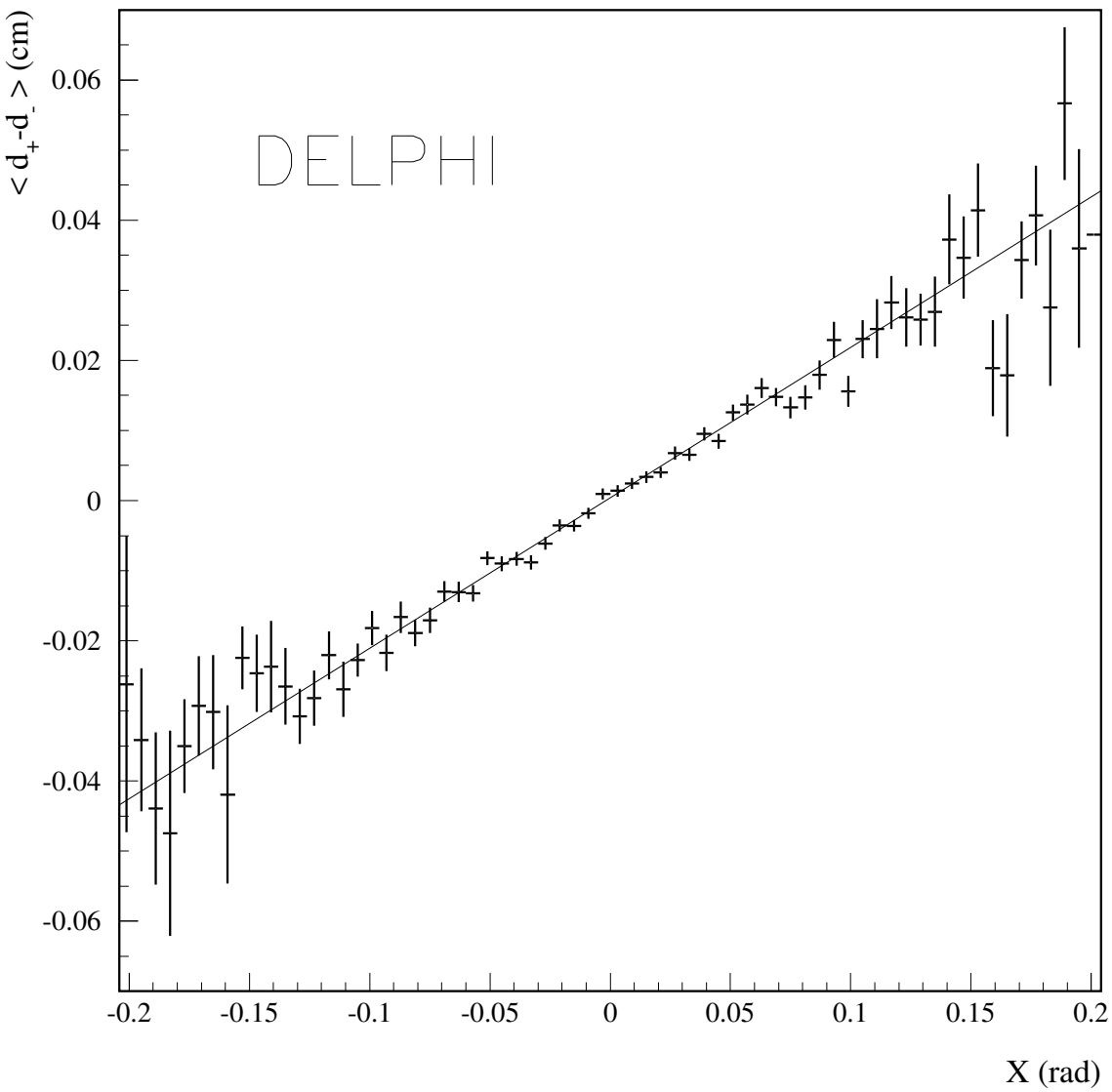

Figure 1: Average value of $d_+ - d_-$ for slices of the X variable defined in the text. The solid line shows the best fit which was performed on an event by event basis.

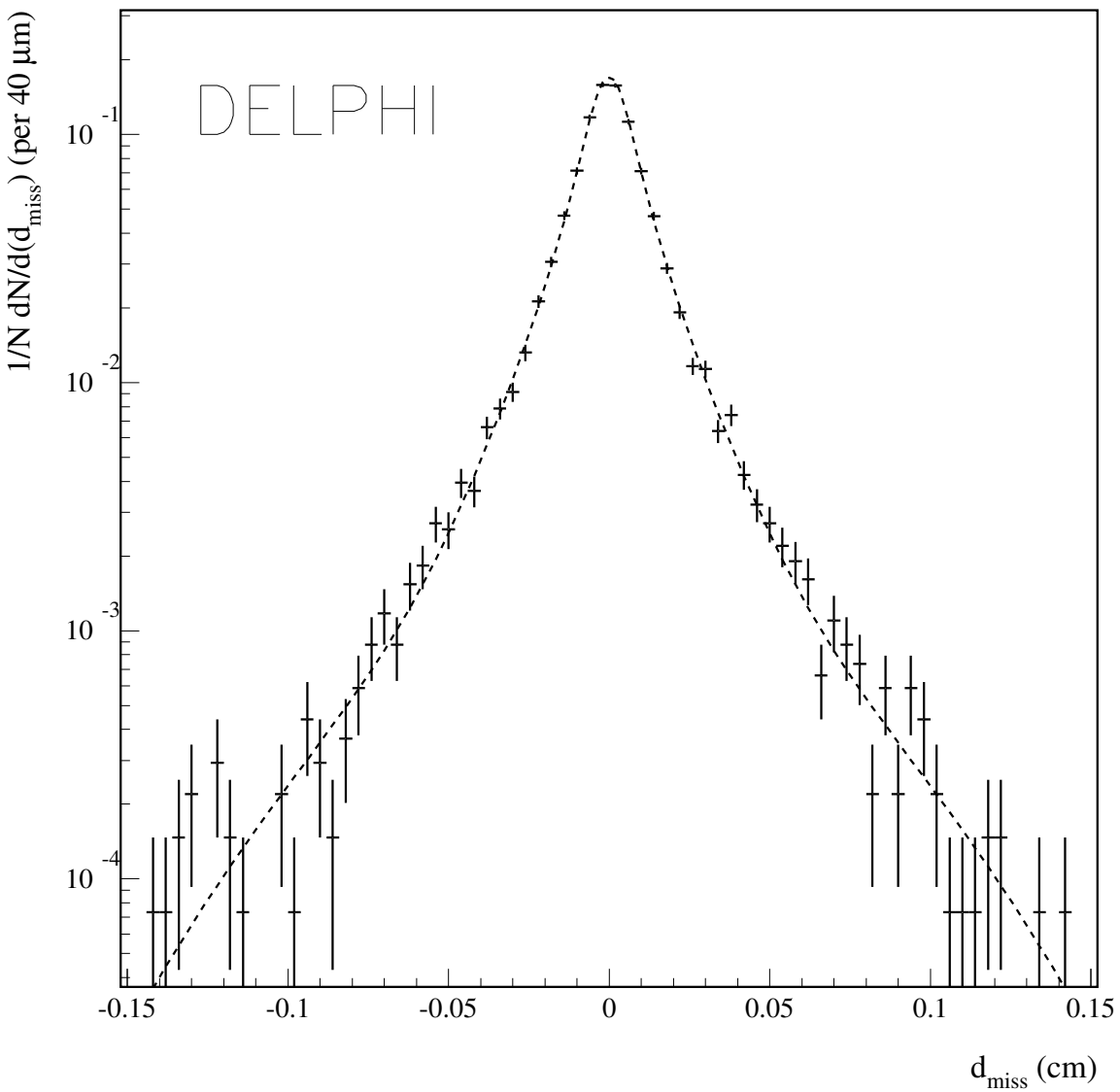

Figure 2: The tau miss distance distribution. The dashed line is the best fit from which the tau lifetime was determined.

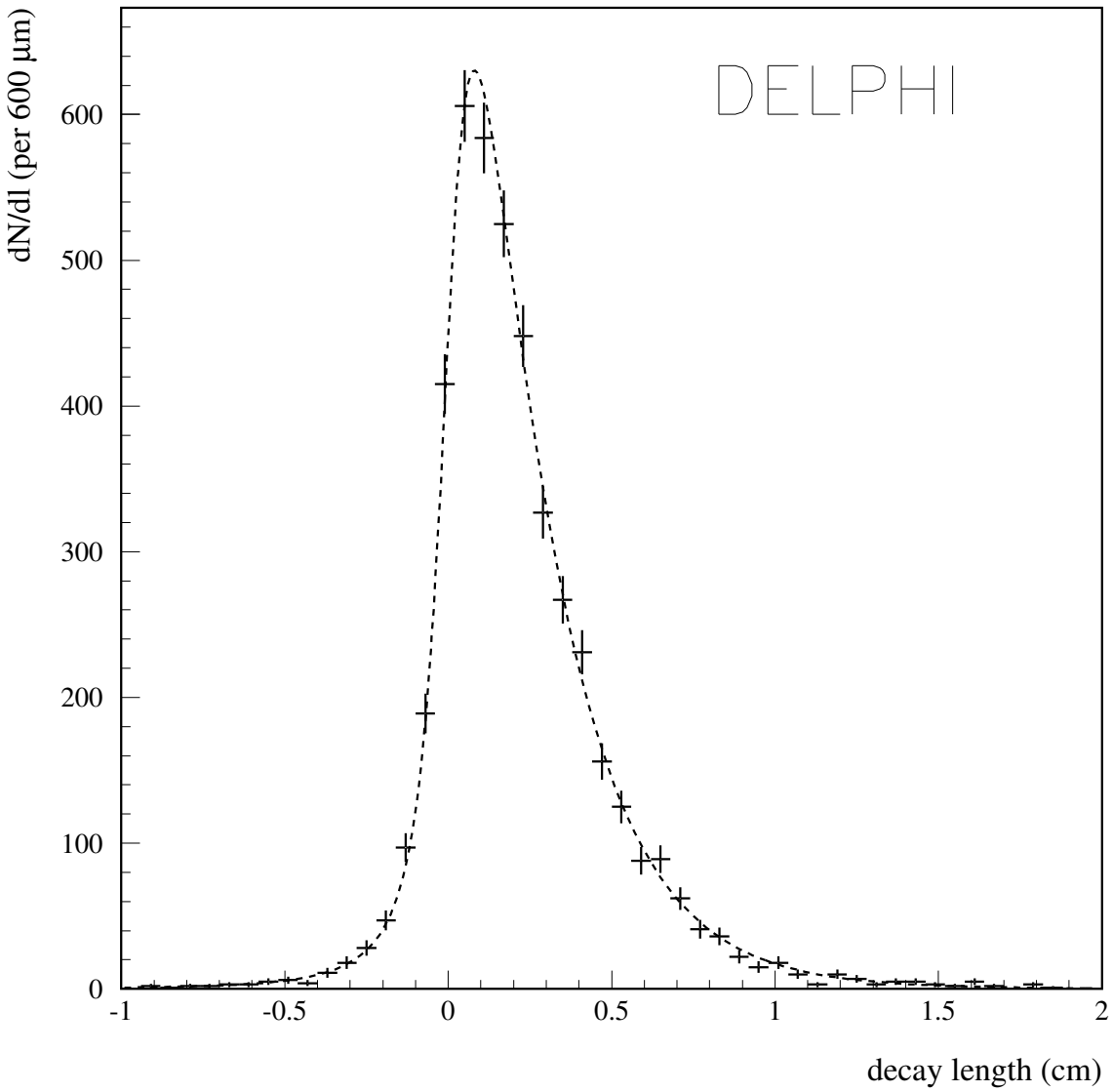

Figure 3: The observed decay length distribution for three-prong taus using the vertex method. The superimposed curve is the result of the maximum likelihood fit as described in the text.